

Supporting Information for

Band Engineering and Morphology Control of Oxygen-incorporated Graphitic Carbon Nitride Porous Nanosheets for Highly Efficient Photocatalytic Hydrogen Evolution

Yunyan Wu^{1, 2, #}, Pan Xiong^{1, #}, Jianchun Wu^{2, 3}, Zengliang Huang², Jingwen Sun¹, Qinjin Liu², Xiaonong Cheng², Juan Yang^{1, 2, *}, Junwu Zhu^{1, *}, Yazhou Zhou^{2, *}

¹Key Laboratory for Soft Chemistry and Functional Materials, Ministry of Education, Nanjing University of Science and Technology, Nanjing 210094, China

²School of Materials Science and Engineering, Jiangsu University, Zhenjiang 212013, China

³Institute of Nuclear Science and Technology, Sichuan University, Chengdu 610064, China

#Yunyan Wu and Pan Xiong have contributed equally to this work

*Corresponding authors. E-mail: yangjuan6347@mail.ujs.edu.cn (J. Yang); zhujw@njust.edu.cn (J. Zhu); yazhou@ujs.edu.cn (Y. Zhou)

S1 Quantum Efficiency Calculations

The apparent quantum yield (AQY) for hydrogen evolution was measured under monochromatic light irradiation (400, 420, 435, and 450 nm) using a 300W Xenon lamp with specific band-pass filters. Depending on the amount of hydrogen produced in one hour, the AQY was calculated from Eqs. (S1)-(S4):

$$\text{AQY} = \frac{\text{Number of evolved hydrogen molecules} \times 2}{\text{Number of incident photons}} \times 100\% \quad (\text{S1})$$

$$\text{Number of evolved hydrogen molecules} = 2 \times M \times N_A \quad (\text{S2})$$

$$\text{Number of incident photons} = \frac{E \times \lambda}{h \times c} \times 100\% \quad (\text{S3})$$

$$\text{AQY} = \frac{2 \times M \times N_A \times h \times c}{S \times P \times \lambda \times t} \times 100\% \quad (\text{S4})$$

Where, M is the mole number of hydrogen molecules (mol), N_A is Avogadro constant ($6.022 \times 10^{23} \text{ mol}^{-1}$), h is Plank constant ($6.626 \times 10^{-34} \text{ J S}$), c is the speed of light ($3 \times 10^8 \text{ m s}^{-1}$), λ is the monochromatic light wavelength (m), P is the average intensity of irradiation, S is the irradiation area (cm^2), and t is the photoreaction time (s).

Table S1 Calculated apparent quantum efficiency (AQE) at different wavelengths

Wavelength	H ₂ Evolved (μmol)	Light Intensity	AQE
λ=400nm	60.95	12.53 mW	26.96%
λ=420nm	10.88	13.41 mW	4.28%
λ=435nm	4.42	14.55 mW	1.55%
λ=450nm	0	15.12 mW	0%

$$AQE(\%) = \frac{\text{the number of reacted electrons}}{\text{the number of incident photos}} \times 100\% = \frac{2 \times \text{the number of evolved H}_2 \text{ molecules}}{N} \times 100\% =$$

$$= \frac{2NAc}{N} \quad (N = \frac{E\lambda}{hc} = \frac{Pt\lambda}{hc})$$

C: H_2 production amount

N_A : Avogadro constant

P: Light intensity

t: Photocatalytic reaction time

λ : The wavelength of light

h: Planck constant

c: The speed of light

(a) $\lambda = 400 \text{ nm}$

$$N = \frac{E\lambda}{hc} = \frac{12.53 \times 10^{-3} \times 3 \times 3600 \times 400 \times 10^{-9}}{6.626 \times 10^{-34} \times 3 \times 10^8} = 2.722 \times 10^{20}$$

$$AQE = \frac{\text{the number of reacted electrons}}{\text{the number of incident photos}} \times 100\% = \frac{2 \times \text{the number of evolved H}_2 \text{ molecules}}{N} \times 100\% =$$

$$\frac{2 \times 6.02 \times 10^{23} \times 60.95 \times 10^{-6}}{2.722 \times 10^{20}} = 26.96\%$$

(b) $\lambda = 420 \text{ nm}$

$$N = \frac{E\lambda}{hc} = \frac{13.41 \times 10^{-3} \times 3 \times 3600 \times 420 \times 10^{-9}}{6.626 \times 10^{-34} \times 3 \times 10^8} = 3.0598 \times 10^{20}$$

$$AQE = \frac{\text{the number of reacted electrons}}{\text{the number of incident photos}} \times 100\% = \frac{2 \times \text{the number of evolved H}_2 \text{ molecules}}{N} \times 100\% =$$

$$\frac{2 \times 6.02 \times 10^{23} \times 10.88 \times 10^{-6}}{3.0598 \times 10^{20}} = 4.28\%$$

(c) $\lambda = 435 \text{ nm}$

$$N = \frac{E\lambda}{hc} = \frac{14.55 \times 10^{-3} \times 3 \times 3600 \times 435 \times 10^{-9}}{6.626 \times 10^{-34} \times 3 \times 10^8} = 3.438 \times 10^{20}$$

$$AQE = \frac{\text{the number of reacted electrons}}{\text{the number of incident photos}} \times 100\% = \frac{2 \times \text{the number of evolved H}_2 \text{ molecules}}{N} \times 100\% =$$

$$\frac{2 \times 6.02 \times 10^{23} \times 4.42 \times 10^{-6}}{3.438 \times 10^{20}} = 1.55\%$$

(d) $\lambda = 450 \text{ nm}$

$$N = \frac{E\lambda}{hc} = \frac{15.12 \times 10^{-3} \times 3 \times 3600 \times 450 \times 10^{-9}}{6.626 \times 10^{-34} \times 3 \times 10^8} = 3.697 \times 10^{20}$$

$$AQE = \frac{\text{the number of reacted electrons}}{\text{the number of incident photos}} \times 100\% = \frac{2 \times \text{the number of evolved H}_2 \text{ molecules}}{N} \times 100\% =$$

$$\frac{2 \times 6.02 \times 10^{23} \times 0 \times 10^{-6}}{3.697 \times 10^{20}} = 0\%$$

S2 Supplementary Tables and Figures

Table S2 XPS comparison of element contents of the different samples

Sample type	N content (at%)	O content (at%)	C content (at%)
OCN -1	60.29	0.84	38.86
OCN -2	59.88	1.02	39.10
OCN -3	59.07	1.62	39.31
OCN -4	58.04	2.07	39.88

Table S3 O bond proportions of the different samples

Sample type	O ₂ content (%)	H ₂ O content (%)	C-O content (%)
OCN -1	23.12	47.45	29.42
OCN -2	19.62	44.66	35.71
OCN -3	15.83	42.52	41.63
OCN -4	14.63	42.46	42.91

Table S4 H₂ evolution rate of other reported CN-based photocatalysts

Composite type	Dopant /cocatalysts	Reactant solution and sacrificial agent	Light source	Activity ($\mu\text{mol g}^{-1}\text{h}^{-1}$)	Refs.
NiMo/g-C ₃ N ₄	1 wt% Pt	100 mL aqueous solution, TEOA (10 vol%)	Xe-lamp (300 W), $\lambda > 420$ nm	1785	[S1]
MS-550	3 wt% Pt	100 mL aqueous solution, TEOA (10 vol%)	Xe-lamp (300 W), $\lambda > 420$ nm	661	[S2]
T-CN	3 wt% Pt	100 mL aqueous solution, TEOA (10 vol%)	Xe-lamp (300 W), $\lambda > 420$ nm	332	[S3]
CN-Na-7	3 wt% Pt	100 mL aqueous solution, TEOA (10 vol%)	Xe-lamp (300 W), $\lambda > 420$ nm	169	[S4]
CNQ680	3 wt% Pt	300 mL aqueous solution, TEOA (10vol%)	Xe-lamp (300 W), $\lambda > 440$ nm	310	[S5]
U-CN-6	3 wt% Pt	100 mL aqueous solution, TEOA (10 vol%)	300 W Xenon lamp, $\lambda > 420$ nm	812	[S6]
g-C ₃ N ₄ @PDA	3 wt% Pt	100 mL aqueous solution, TEOA (10 vol%)	300 W Xe-lamp, $\lambda > 420$ nm	377.7	[S7]
3DCN1	3 wt% Pt	100 mL aqueous solution, TEOA (10 vol%)	300 W Xenon lamp, $\lambda > 420$ nm	1681	[S8]
P-DCN	3 wt% Pt	100 mL aqueous solution, TEOA (10 vol%)	300W Xeon-lamp, $\lambda > 420$ nm	2092	[S9]
CNU _{0.075}	1 wt% Pt	100 mL aqueous solution, TEOA (10 vol%)	300W Xenon arc lamp, $\lambda > 420$ nm	1003.9	[S10]
Co(Mo-Mo ₂ C)/g-C ₃ N ₄	2 wt% Pt	10 mL aqueous solution, TEOA (20 vol%)	300W Xenon arc lamp, $\lambda > 420$ nm	4291	[S11]
OCN	3 wt% Pt	100 mL aqueous solution, TEOA (10 vol%)	300W Xenon arc lamp, $\lambda > 420$ nm	3519.6	Our Work

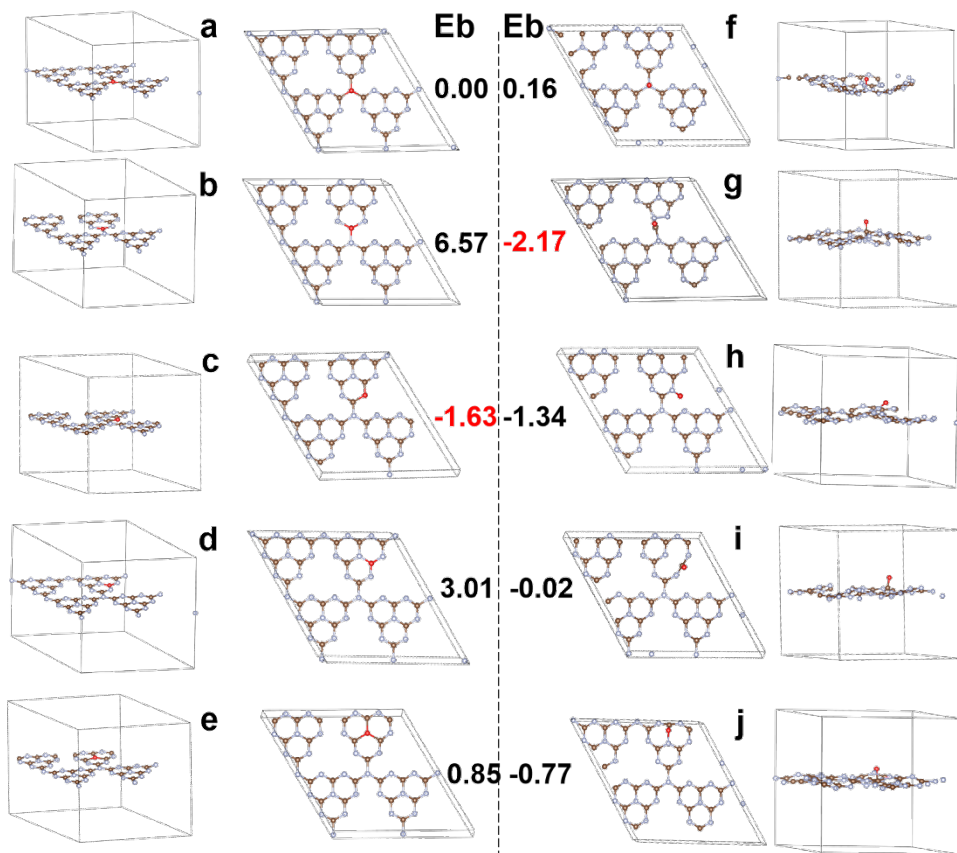


Fig. S1 a-e Optimized atomic structure view and energy of O-doped g-C₃N₄ and **f-j** O-adsorbed g-C₃N₄

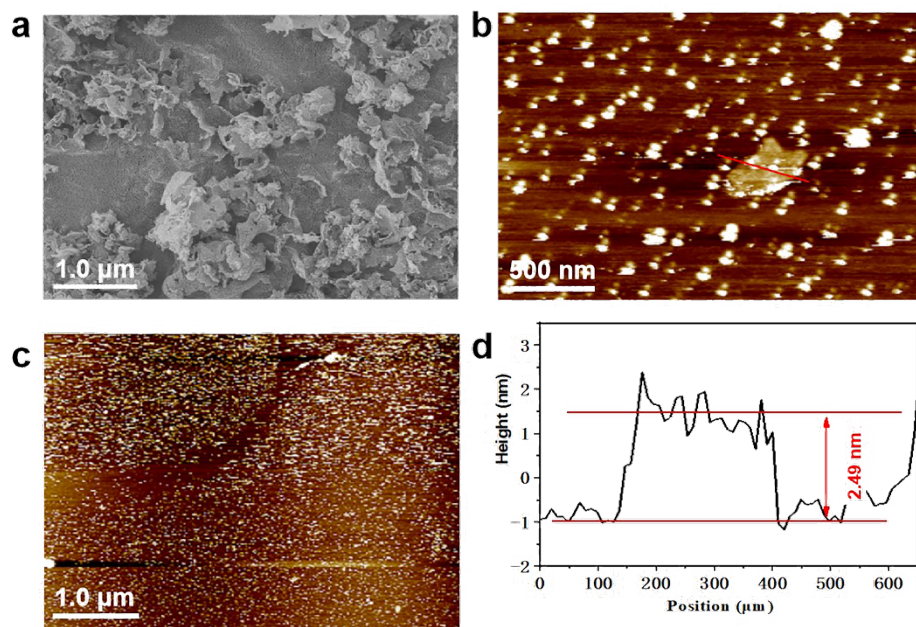


Fig. S2 a SEM, **b-d** AFM images of OCN-4

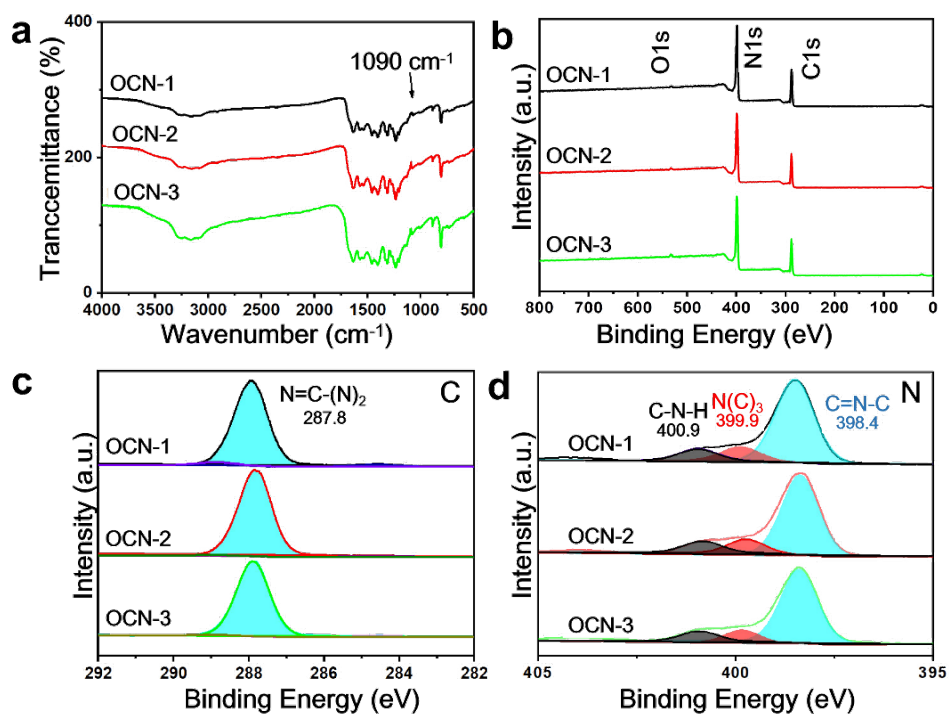


Fig. S3 **a** FT-IR, **b** survey, **c-d** C1s and N1s XPS spectra of OCN

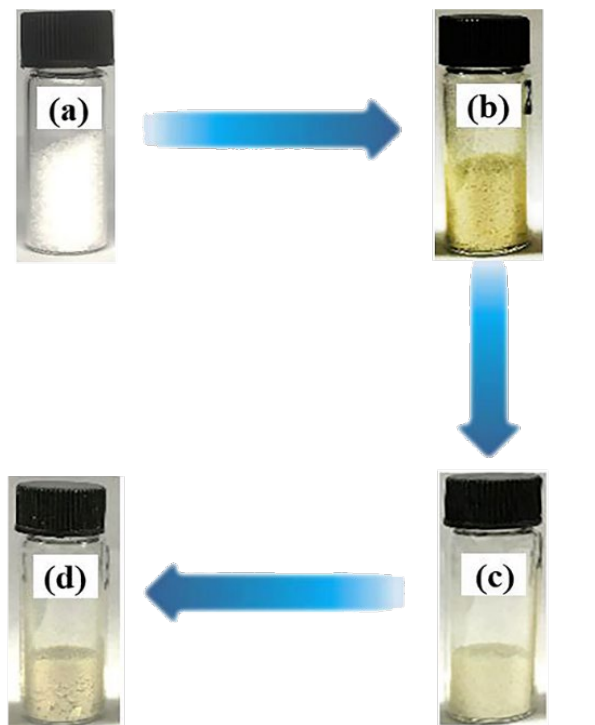


Fig. S4 **a-d** Digital photographs of powders: **a** precursor urea, **b** OCN-1, **c** OCN-2, **d** OCN-3

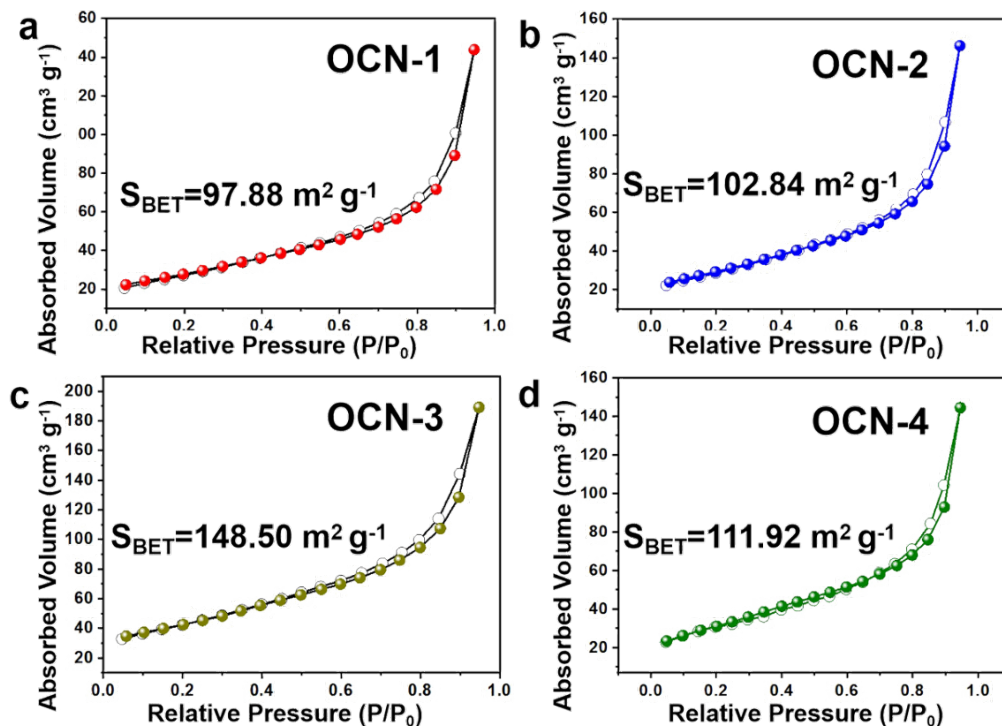


Fig. S5 a-d Nitrogen adsorption/desorption isotherms of **a** OCN-1, **b** OCN-2, **c** OCN-3, **d** OCN-4

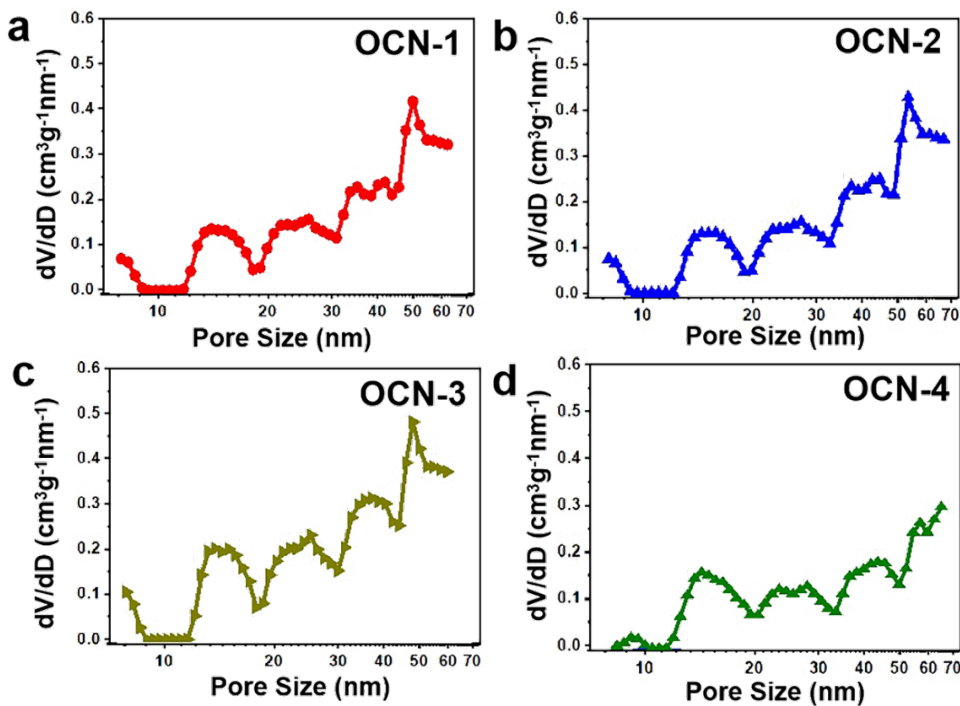


Fig. S6 a-d Pore size distribution curves of **a** OCN-1, **b** OCN-2, **c** OCN-3, **d** OCN-4

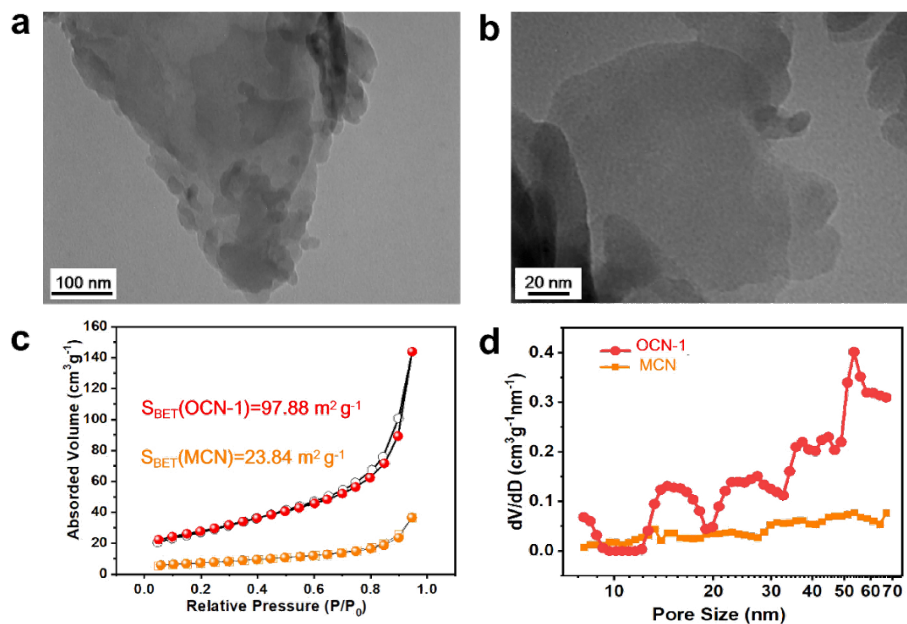


Fig. S7 **a-b** TEM images of MCN, **c** nitrogen adsorption/desorption isotherms and **d** pore size distribution curves of OCN-1, MCN

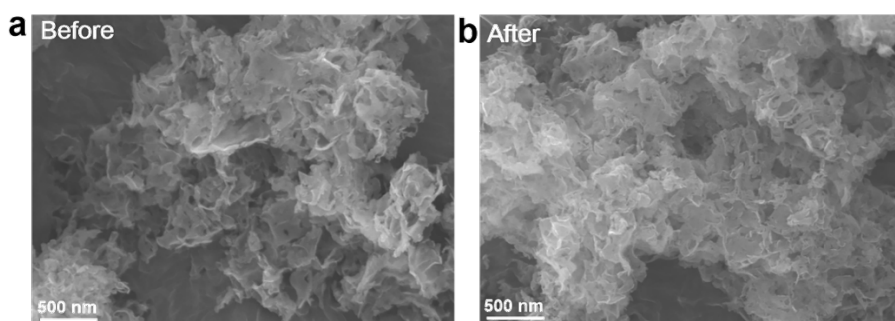


Fig. S8 **a-b** SEM images of OCN-3 before and after cyclic photocatalytic H_2 evolution tests

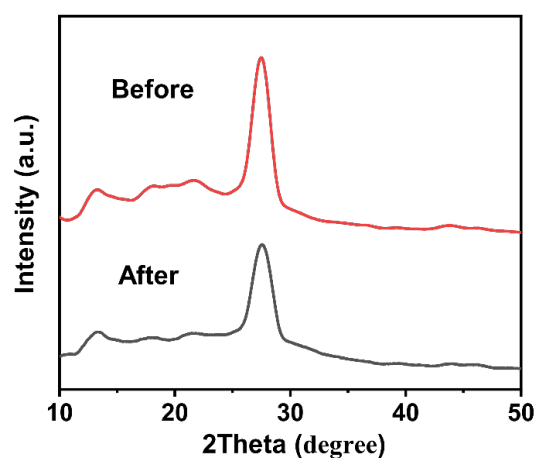


Fig. S9 XRD patterns of OCN-3 before and after cyclic photocatalytic H_2 evolution tests

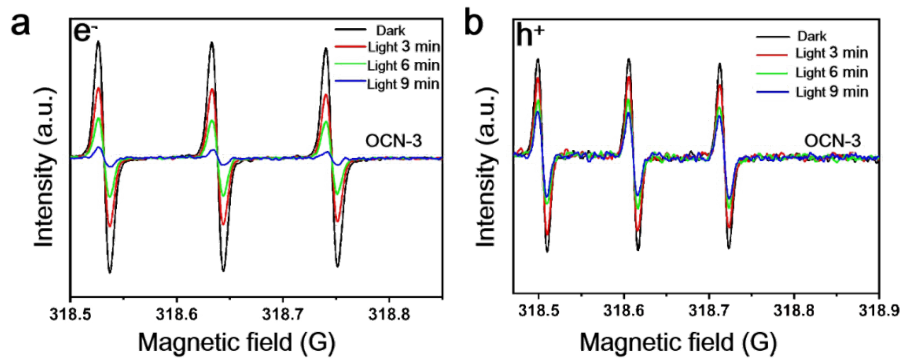


Fig. S10 a-b ESR spectra of e^- and h^+ for various times of OCN-3 under visible light irradiation

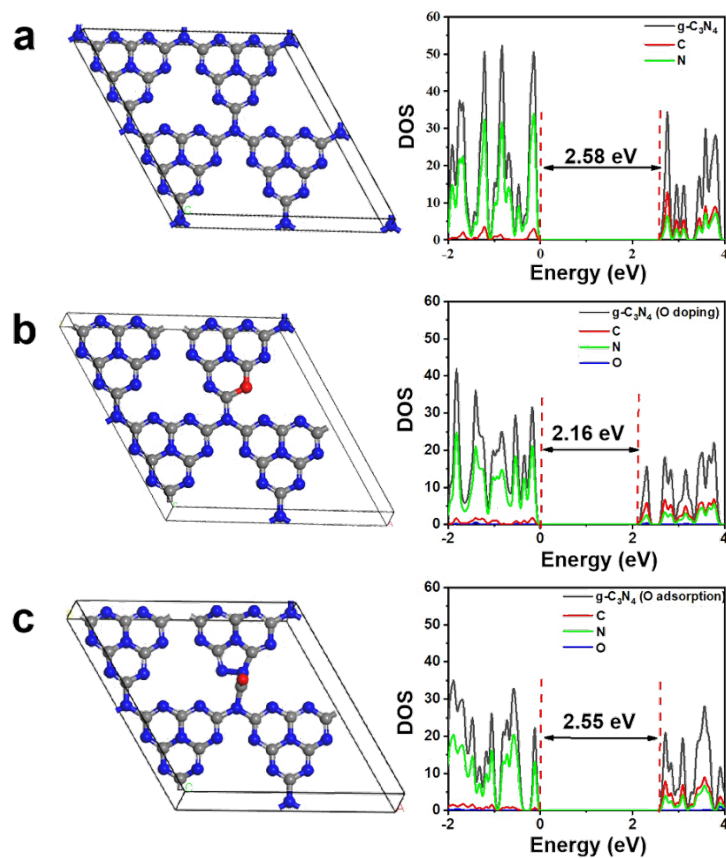


Fig. S11 a-c Density of state (DOS) of **a** pristine $g\text{-C}_3\text{N}_4$, **b** O-doped $g\text{-C}_3\text{N}_4$ and **c** O-adsorbed $g\text{-C}_3\text{N}_4$

Supplementary References

- [S1] X. Han, D. Xu, L. An, C. Hou, Y. Li et al., Ni-Mo nanoparticles as co-catalyst for drastically enhanced photocatalytic hydrogen production activity over $g\text{-C}_3\text{N}_4$. *Appl. Catal. B: Environ.* **243**, 136-144 (2019).
<https://doi.org/10.1016/j.apcatb.2018.10.003>

- [S2] J. Yang, Y. Liang, K. Li, G. Yang, K. Wang et al., One-step synthesis of novel K⁺ and cyano groups decorated triazine-/heptazine-based g-C₃N₄ tubular homojunctions for boosting photocatalytic H₂ evolution. *Appl. Catal. B: Environ.* **262**, 118252 (2020). <https://doi.org/10.1016/j.apcatb.2019.118252>
- [S3] J. Yang, Y. Liang, K. Li, G. Yang, K. Wang et al., Cyano and potassium-rich g-C₃N₄ hollow tubes for efficient visible-light-driven hydrogen evolution. *Catal. Sci. Technol.* **9**, 3342-3346 (2019). <https://doi.org/10.1039/C9CY00925F>
- [S4] Y. Shang, Y. Ma, X. Chen, X. Xiong, J. Pan, Effect of sodium doping on the structure and enhanced photocatalytic hydrogen evolution performance of graphitic carbon nitride. *Molecular Catal.* **433**, 128-135 (2017). <https://doi.org/10.1016/j.mcat.2016.12.021>
- [S5] P. Niu, M. Qiao, Y. Li, L. Huang, T. Zhai, Distinctive defects engineering in graphitic carbon nitride for greatly extended visible light photocatalytic hydrogen evolution. *Nano Energy* **44**, 73-81 (2018). <https://doi.org/10.1016/j.nanoen.2017.11.059>
- [S6] C. Dong, Z. Ma, R. Qie, X. Guo, C. Li et al., Morphology and defects regulation of carbon nitride by hydrochloric acid to boost visible light absorption and photocatalytic activity. *Appl. Catal. B: Environ.* **217**, 629-636 (2017). <https://doi.org/10.1016/j.apcatb.2017.06.028>
- [S7] H. Wang, Q. Lin, L. Yin, Y. Yang, Y. Qiu et al., Biomimetic design of hollow flower-like g-C₃N₄@PDA organic framework nanospheres for realizing an efficient photoreactivity. *Small* **15**, 1900011 (2019). <https://doi.org/10.1002/smll.201900011>
- [S8] J. Sun, F. Yao, L. Dai, J. Deng, H. Zhao et al., Task-specific synthesis of 3D porous carbon nitrides from the cycloaddition reaction and sequential self-assembly strategy toward photocatalytic hydrogen evolution. *ACS Appl. Mater. Inter.* **12**, 40433-40442 (2020). <https://doi.org/10.1021/acsami.0c14097>
- [S9] D. Zhang, Y. Guo, Z. Zhao, Porous defect-modified graphitic carbon nitride via a facile one-step approach with significantly enhanced photocatalytic hydrogen evolution under visible light irradiation. *Appl. Catal. B: Environ.* **226**, 1-9 (2018). <https://doi.org/10.1016/j.apcatb.2017.12.044>
- [S10] Q. Xu, B. Zhu, B. Cheng, J. Yu, M. Zhou et al., Photocatalytic H₂ evolution on graphdiyne/g-C₃N₄ hybrid nanocomposites. *Appl. Catal. B: Environl.* **255**, 117770 (2019). <https://doi.org/10.1016/j.apcatb.2019.117770>
- [S11] Y. Zheng, J. Dong, C. Huang, L. Xia, Q. Wu et al., Co-doped Mo-Mo₂C cocatalyst for enhanced g-C₃N₄ photocatalytic H₂ evolution. *Appl. Catal. B: Environl.* **260**, 118220 (2020). <https://doi.org/10.1016/j.apcatb.2019.118220>